Flood Simulation by Euler-Lagrangian Method

Ivan Botev　　Masayasu Ito

オイラー・ラグランジュ法による洪水シミュレーション

イヴァン　ボテヴ　　伊　藤　雅　保

概　　要

水深方向に平均化したナビエ・ストークス方程式を基礎式とする混合オイラー・ラグランジュ（EL）法を用いて，長方形貯水池での洪水の2次元数値シミュレーションを実施した。EL法では反復計算の必要がなく，境界条件の扱いも比較的簡便である。本手法を用いて貯水池の水位および流速の時間変化をシミュレーションした結果は，浅水理論や1次元解析の結果と定性的に一致しており，物理的な現象をよく再現していることがわかった。洪水シミュレーションの結果，EL法は非定常性の強い急峻な流れの問題についても十分信頼性のあることを確認した。

Abstract

A two-dimensional combined Euler-Lagrangian (EL) method based on simplified depth-averaged Navier-Stokes equations was adopted for a flood simulation study. The lack of iterative procedures and convergence-related problems were among the reasons for adopting this method. Calculations were carried out on an artificial rectangular reservoir. The results illustrate the rates of variation of water elevation and flow velocity inside the reservoir, and these were compared with Stokes' analytical solution and a one-dimensional numerical solution. It is concluded that the results obtained by the EL method are in conformity with the physics of the simulated phenomena, yielding a lower rate of variation of water elevation inside the reservoir when compared with the one-dimensional results. The EL method is reliable in handling rapidly-varying flows, while further refinement of the method is possible.

1. Introduction

Flood and heavy rainfall are at the origin of serious accidents in the engineering practice. To prevent tragic consequences of flood accidents, accident prediction and prevention studies rely mostly on numerical methods.

The combined Euler-Lagrangian (EL) method was adopted in the present study to simulate a hypothetical flood accident. This is an attractive and promising method that has a good capacity to handle rapidly varied flow and permits an easy treatment of initial and boundary conditions. In addition, the EL method avoids time-consuming iterative solutions and convergence related problems. The results of the study, conducted for the case of a rectangular reservoir, illustrate the rate of variation of some important parameters, such as water elevation and flow velocity, during the accident. Based on these results, appropriate measures could be conceived in order to secure against flooding the dikes of the reservoir and the structures inside it.

2. Numerical Method and Flow Model

The EL method is implemented in two horizontal dimensions. The fluid is represented as a set of moving fluid particles of fixed volume. First, at each time step, Lagrangian positions and velocities for all moving fluid particles are determined. Then, Eulerian depth of flow and velocity field, defined with respect to a two-dimensional grid overlaying the computational domain, are evaluated based upon the distribution of fluid particles in the domain. It should be noted that velocity is treated as both, a Lagrangian

(in respect to moving fluid particles) and Eulerian (in respect to a fixed grid in the computational domain) variable, playing the role of interface between Lagrangian and Eulerian approaches. For instance, flow velocity at each grid point is calculated as the average velocity of all fluid particles present in the rectangular grid cell having the grid point at its center. Similarly, flow depth is proportional to the number of fluid particles present in each cell. The average flow depth over the cell is calculated from the number of fluid particles within the cell, the volume of each particle and the size of the cell.

The governing set of equations adopted for the flow model consists of the depth-integrated Navier-Stokes equations in the form:

$$\frac{\partial h}{\partial t}=-\nabla\cdot(h\mathrm{U}) \qquad \cdots\cdots(1)$$

$$\frac{\partial \mathrm{U}}{\partial t}+\frac{\partial H}{\partial t}\frac{\mathrm{U}}{h}\alpha+(\mathrm{U}\cdot\nabla)\mathrm{U}\beta+\frac{\mathrm{U}}{h}\left\{\frac{\partial H}{\partial t}\gamma_1+(\mathrm{U}\cdot\nabla)Z\gamma_2+(\mathrm{U}\cdot\nabla)h\gamma_3\right\}=-g\nabla H+\frac{\mu}{\rho}\nabla^2\mathrm{U}+2\frac{\mu}{\rho}\frac{1}{h}(\nabla\mathrm{U}\cdot\nabla h\varepsilon)+\frac{\mu}{\rho}\frac{1}{h}\mathrm{U}\nabla^2(h\varepsilon)+\frac{\mu}{\rho}\frac{\mathrm{U}}{\rho h^2}\phi \qquad \cdots\cdots(2)$$

where

- U = $\bar{u}\mathrm{i}+\bar{v}\mathrm{j}$ vertically averaged horizontal velocity
- $\bar{u}$, $\bar{v}$ = components of the averaged horizontal velocity
- i, j = vectors of unit length along x and y axes
- g = acceleration of gravity
- H = elevation of free water surface
- h = $H-Z$ = flow depth
- t = time
- Z = topographic elevation
- μ = viscosity of fluid
- ρ = density of fluid

The first equation is the depth-averaged continuity equation involving the horizontal flow velocity and the depth of the fluid confined between a rigid boundary below and a free-surface flow above. The second equation represents the depth-integrated forms of the momentum equations in the x and y directions, combined in a single expression. Coefficients α through ϕ in Equation (2) depend on the shape of the velocity profile. A comprehensive analysis and a detailed description of the model used as a prototype for the present study can be found in[2].

Considering a hypothetical accident, a situation where no experimental results for reference are available, the numerical results presented in Section 5 were devised with economy of computing effort in mind and emphasis on the concept in solving a specific problem rather than accuracy of the solution. Accordingly, β was taken equal to unity and the rest of the coefficients in Equation (2) were set equal to zero. Equation (2) thus becomes

$$\frac{\partial \mathrm{U}}{\partial t}+(\mathrm{U}\cdot\nabla)\mathrm{U}=\frac{Du}{Dt}=-g\nabla H+\frac{f_2}{\rho}\nabla^2\mathrm{U}-f_1\frac{\mathrm{U}|\mathrm{U}|}{h} \qquad \cdots\cdots(3)$$

As the above simplification would imply that there is no horizontal friction within the flow and consequently the velocity profile is constant with depth, bottom friction proportional to the square of the depth-averaged flow velocity was reintroduced in the model in order for the flow to be realistic. A more detailed comparative study that will gradually include all coefficients is in progress. In Equation (3), $f_1=gn^2/h^{1/3}$ is the bottom friction coefficient and n is Manning's roughness coefficient.

As suggested in[2], the water viscosity μ in Equation (2) was replaced by a lateral friction coefficient f_2 that represents the effect of shear between portions of fluid of different horizontal velocities. The calibration of f_2 is discussed in Section 4.

Equation (3) expressed in difference form is used to update velocities of each fluid particle at each time increment and the position of each fluid particle is determined from

$$\mathrm{X}_{k+1,t}=\mathrm{X}_{k,t}+(\mathrm{U}_{k,t}+\mathrm{U}_{k,t+1})\Delta t/2 \qquad \cdots\cdots(4)$$

where

- $\mathrm{X}_{k,t}$ = position of fluid particle k at time t
- $\mathrm{X}_{k,t+1}$ = position of fluid particle k at time $t+1$
- $\mathrm{U}_{k,t}$ = velocity of fluid particle k at time t
- $\mathrm{U}_{k,t+1}$ = velocity of fluid particle k at time $t+1$
- Δt = computational time step

3. Case Study

Dikes form a rectangular $B\times L\times H=37.5\times97.5\times7.0\ m$ reservoir of trapezoidal cross-section (all dimensions measured from top of dikes) with uniform bottom slope $i=0.01$ (Fig. 1 and 2). A bulkhead, designed to withstand a water head of 6.70 m, is erected at the right end of the reservoir. The reservoir is initially empty. The problem to be solved is formulated as follows: assume that the reservoir is flooded and simulate the variation of water elevation and flow velocity inside the reservoir corresponding to approximately 1 m increase above the design head of the bulkhead.

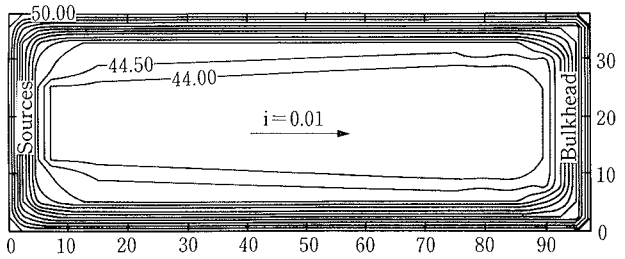

Fig. 1 Horizontal plan of the reservoir

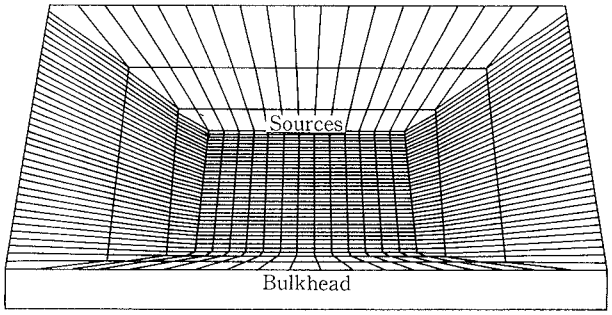

Fig. 2 Perspective view of the reservoir

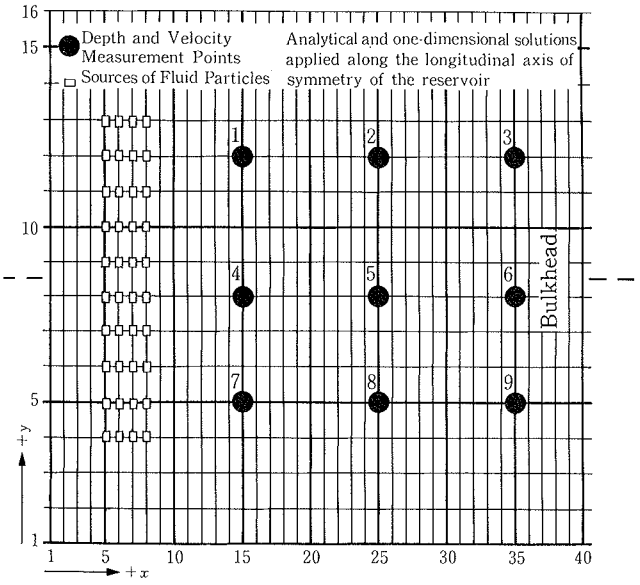

Fig. 3 Computational grid for EL method

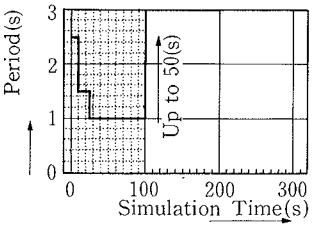

Fig. 4 Relationship between release period of fluid particles at sources and simulation time

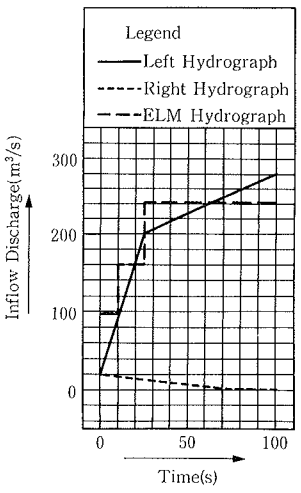

Fig. 5 Water discharge hydrographs for 1- and 2-D solutions

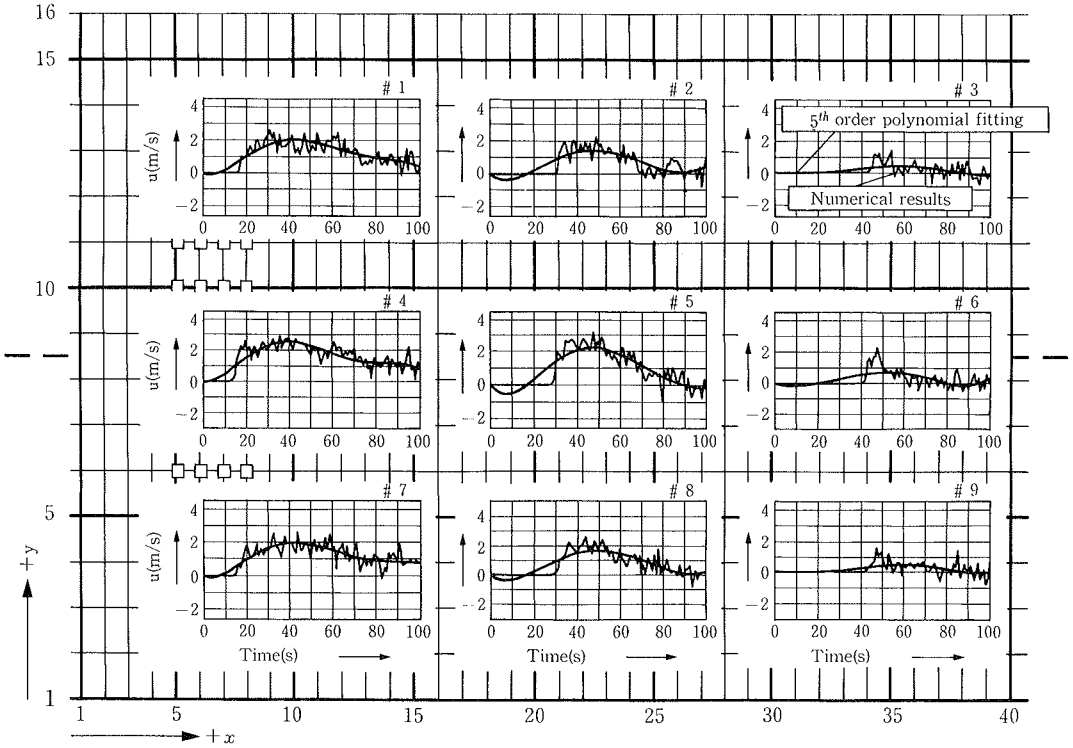

Fig. 6 U-velocity component variation at monitoring points

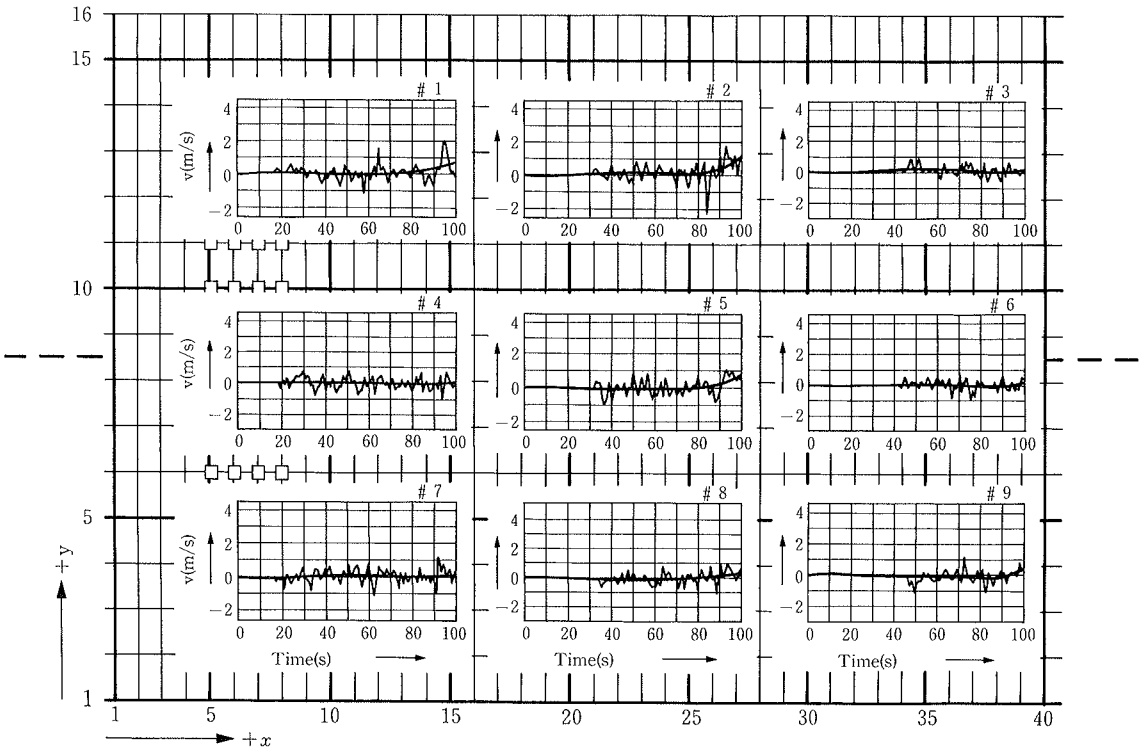

Fig. 7　V-velocity component variation at monitoring points

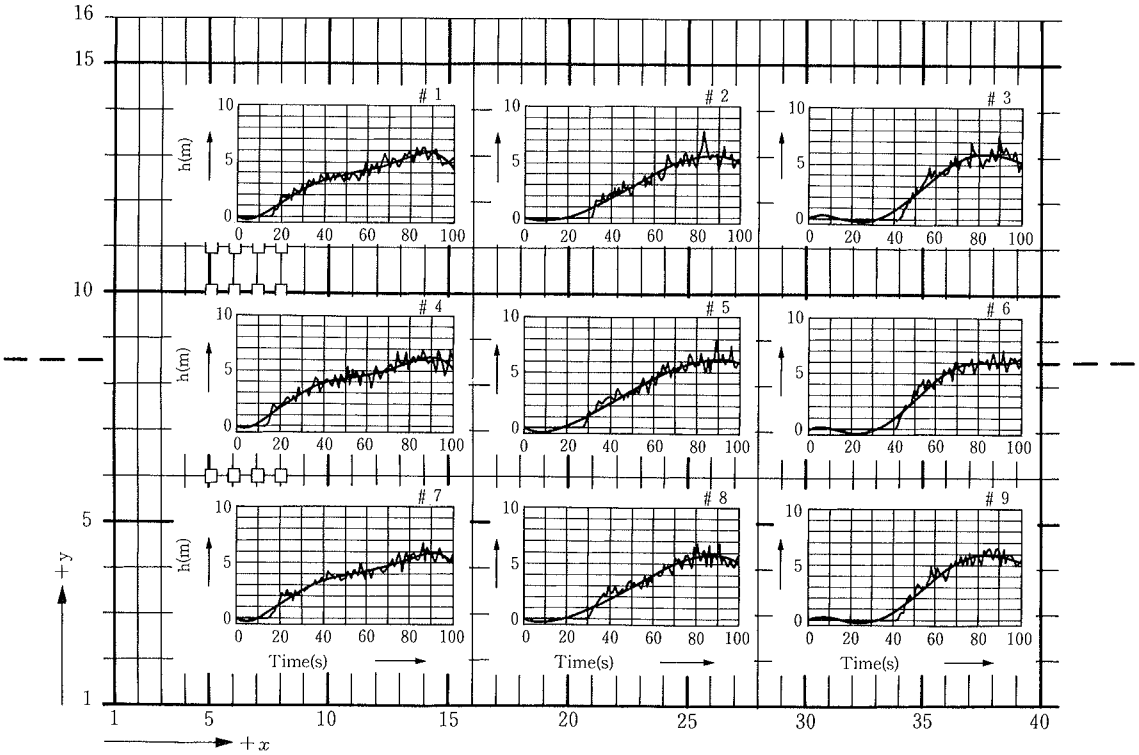

Fig. 8　Water depth variation at monitoring points

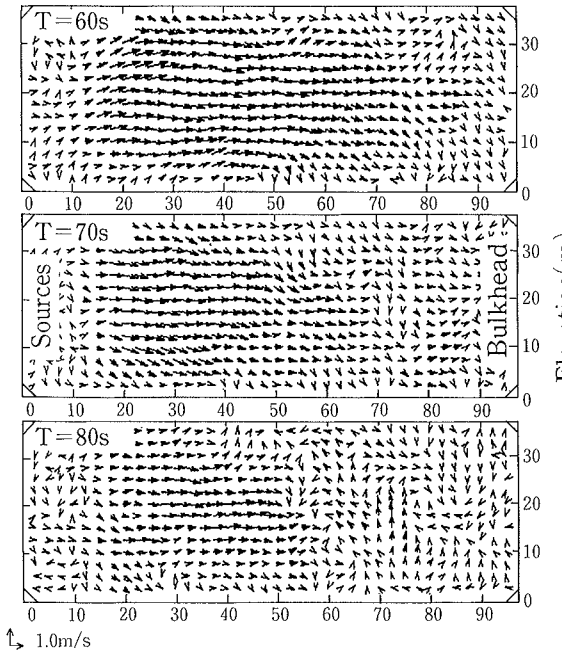

Fig. 9 Velocity field in the reservoir at 10 *s* intervals

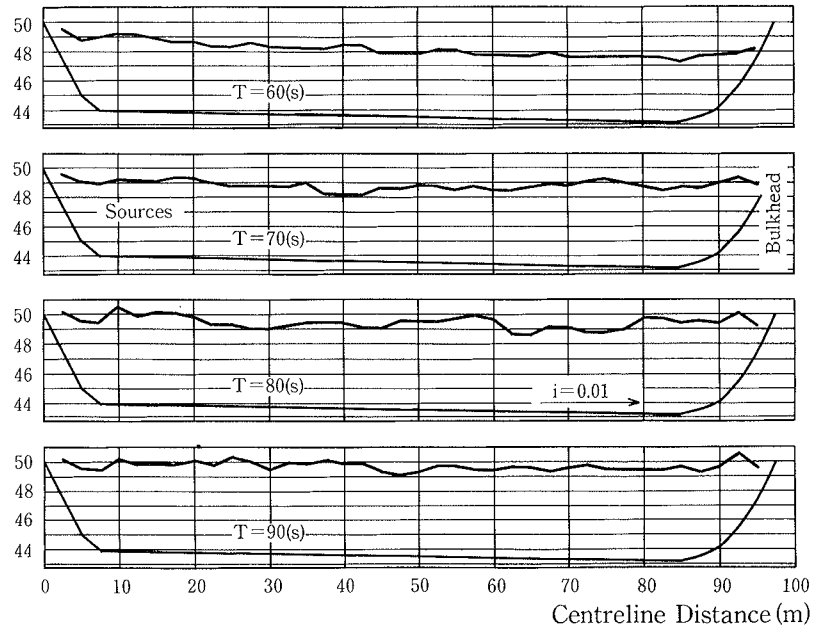

Fig. 10 Water surface profiles along longitudinal axis of symmetry by EL method

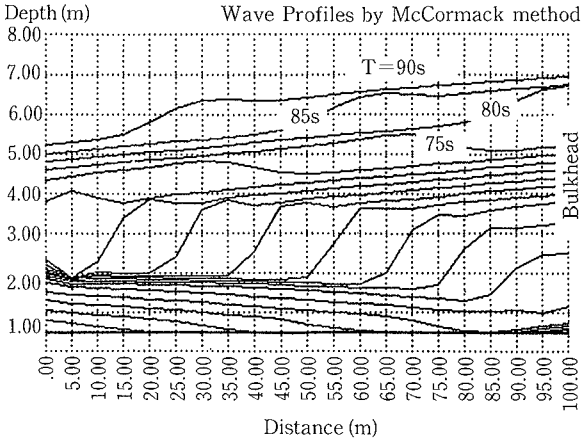

Fig. 11 Water surface profiles along longitudinal axis of symmetry by 1-D solution

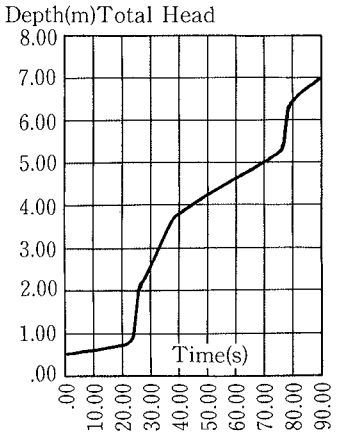

Fig. 12 Total head variation in front of bulkhead by 1-D solution

4. Verification Tests and Calibration of the Model

Two series of verification tests, as prescribed in[2] were carried out ensure that the 2-D EL flow model accords with energy and momentum conservation laws.

In addition, the coefficient of lateral friction f_2 needed to be calibrated so that measured depth-averaged horizontal velocities at different locations in the reservoir could be reproduced satisfactorily by the numerical model. Because experimental data was not available, velocities necessary for the calibration of f_2 were calculated using a 1-D numerical solution based on the full Saint-Venant equations written in conservation form. The equations were discretized by means of Mac-Cormack two-step explicit difference sheme.

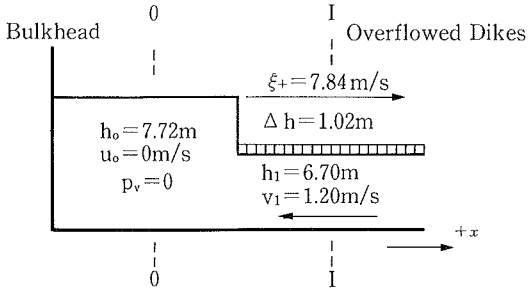

Fig. 13 Reflection of a stream from a rigid wall

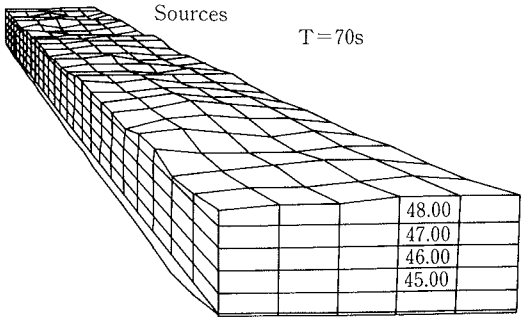

Fig. 14 Water surface along longitudinal axis of symmetry by EL method

5. Results

The reservoir is transformed into a 2-D computational domain using a uniformly spaced ($\Delta x=\Delta y=2.5$ m) 40×16 grid. A unilaterally distorted image of the grid is shown on Fig. 3. A rapidly varied water release is modeled using 160 (4 layers$\times$40) sources of fluid particles concentrated on the left side of the grid. The intensity with which fluid particles are released at the sources is expressed as a release period vs. time relationship (Fig. 4) and the hydrograph on Fig. 5 (thick broken line) respectively. The variation of horizontal velocity components (u, v) and depth (h) at 9 specific grid points were monitored during simulation. Fig. 6, 7 and 8 illustrate these variations. A 5^{th} order polynomial fitting is used to improve the illustration of the numerical results shown by a thin oscillating line. Three consecutive velocity fields are also shown on a horizontal plan of the reservoir in Fig. 9. Water surface profiles drawn along the longitudinal axis of symmetry of the reservoir and corresponding to these velocity fields are illustrated in Fig. 10. All experiments were conducted using fluid particles with a volume of 1.5 m^3 and time step $\Delta t=0.05$ s.

Mac-Cormack numerical solution is illustrated under the form of (1)-longitudinal water surface profiles (along the longitudinal axis of symmetry, perpendicular to the bulkhead) plotted at time intervals of $\Delta t=5$ s (Fig. 11) and (2)-total head variation in front of the bulkhead (Fig. 12). The solution is obtained for a channel of trapezoidal cross-section with the same dimensions as the reservoir. The bottom slope of the channel is 0.01, the lateral slope of the dikes enclosing the channel corresponding to 45°. Manning's roughness coefficient is $n=0.04$, the computational time step and grid interval are respectively $\Delta t=0.5$ s and $\Delta x=5$ m, determined by the stability criterion. For computational reasons, prior to the flooding, initial channel flow with a discharge equivalent to $Q=20$ m^3/s in the right direction is assumed. The flood hydrograph at the left boundary of the channel is modeled according to the solid line shown on Fig. 5. A thin broken line represents a hydrograph of a gradually vanishing outflow at the right boundary respectively.

For reference, a very popular analytical solution given by Stoker[1] and known as *Reflection of a stream from a rigid wall* is illustrated in Fig. 13. The solution is based on the shallow water theory of first order and is a valuable reference for comparison with numerical solutions, since there is a lot of physical insight to be gained through its consideration. For the purpose of the present study, the analytical solution yields a quantitative evaluation of a sudden increase in water depth in front of the bulkhead for a mean velocity u_1, selected among velocities typical for the flow in the reservoir, calculated using the 2-D solution.

The analytical solution is obtained along the longitudinal axis of symmetry of the reservoir. It is assumed that the flow in the reservoir has a mean velocity $u_1=1.20$ m/s and depth $h_1=6.70$ m. Both values are necessary in order to solve the shock equations [1, p. 328]. The value of h_1 is taken equal to the value of the design head for the bulkhead-6.70 m. The celerity ξ_+ of the reflected stream is obtained by solving the first shock equation and taking the largest of the three roots: $\xi_+=7.84$ m/s. The depth in contact with the wall ($h_0=7.72$ m) is obtained from the second shock equation. As observed from Fig. 13, the maximum depth increase in front of the bulkhead is equal to the height of the reflected stream-($\Delta h=1.02$ m).

6. Discussion

It is well understood that the performance of the 2-D EL flow model should be evaluated by means of a comparative study including experimental results or observations conducted on a real event, so that simulated and real time histories could be compared. At this phase of the study, an analytical and one numerical solution provide a basis for comparison.

All three (analytical, 1- and 2-D) solutions simulate a head increase in front of the bulkhead. The analytical solution is restricted by "zero bottom slope" and "no friction" assumptions and can not simulate the time frame of the flow in the reservoir. However, it suggests that the physics of the simulated phenomena are handled satisfactory by the numerical solutions. As seen from Fig. 9 and 10, the variations of water elevation and velocity field in the reservoir testify for the presence of several propagation waves of a bore type in the longitudinal direction of the reservoir. The waves reflect from the bulkhead, superimpose on the incoming waves and are at the origin of severe disturbances of the water surface.

The fact that v-velocity components in the reservoir are approximately equal to zero draws support in favor of using a 1-D solution for the purpose of both, calibration of the coefficient of lateral friction f_2 and comparison with 2-D results. The 1-D Mac-Cormack solution simulates a water head increase in front of the bulkhead that is rather significant in magnitude and sudden in time ($\approx$1.3 m within 5 s, Fig. 12). This result is attributed to the one-dimensionality of the solution. It appears that one-dimensionality does not allow for partial dissipation of the initial disturbance through reflected waves in a lateral direction as it may be observed in the case of the EL solution (Fig. 14). Similarly to the analytical solution, the 1-D solution simulates an almost sudden increase in head. Is case of the 2-D solution however, the head increase is less intensive ($\approx$1.3 m within 10 s, Fig. 8, pt. # 6). Indeed, fluid particles, moving upward and downward along the inclined surface of the dikes, are reflected gradually. Moreover, all particles are interacting with each other, slowing down their course and consequently reducing the velocity of their impact on the bulkhead.

Comparison between the 1- and 2-D solutions shows that they have different time frames. The 1-D solution features two jumps in head variation in front of the bulkhead (Fig. 12). The first jump is at $T=25$ s and the second at $T=75$ s. A rather intense increase in head also occurs between the two jumps.

On the contrary, the 2-D solution (Fig. 8, pt. # 6) simulates a delayed (after $T=40$ s) start in head increase in front of the bulkhead and shows no jumps. The solution is delayed and extended in time when compared with 1-D results.

The head variation in front of the bulkhead plays an important role in its safety analysis. According to the 1-D solution, the increase of head occurs within approximately half of the time interval as calculated by the 2-D solution. Logically, the 1-D solution should be recommended for design purposes to determine the safety margin of the bulkhead. However, when advancing towards reality by means of the 2-D solution, the head increase appears less intense, meaning that the safety margin could be reduced, if necessary.

Finally, the 2-D solution, viewed as an approximation of the real phenomena occurring in the reservoir, appears very close to reality and inspires confidence. The EL method provides a very simple and physically consistent way to specify external and internal boundary conditions by assigning sources of fluid particles (inflow), or authorizing the particles to exit freely (outflow) anywhere around or inside the computational domain. Assigning sources inside the computational domain being as simple as on the external boundaries, it follows that the subdivision of the computational domain into sub-reaches is no longer required in order to specify internal boundary conditions as is traditional in the case of a pure Eulerian formulation. In addition, the uniform distribution of sources over the entire domain accommodates for the simultaneous treatment of such a "horizontally uniform" condition as rainfall, a feature often present during flood related accidents.

7. Conclusion

A computationally challenging 2-D EL method is advocated as an engineering tool in accident prediction and prevention studies. The method appears to have a good capacity to handle rapidly varied flow phenomena under the initial and boundary conditions encountered during flood and rainfall analysis. With a good physics interpretation of the phenomena under investigation and still unfulfilled possibilities for refinement of the solution, the method is viewed as a reliable tool, especially when a supportive experimental study is not feasible. Coupling the 2-D EL method with other 2-D solutions is expected to overcome the difficulties arising from the lack of experimental data

necessary for the calibration of the coefficient of lateral friction. Using several numerical solutions in one case study has the advantage of providing a basis for instructive comparative studies and eliminating random errors in the solutions. Moreover, it provides the solution variety and quality needed to strengthen confidence in accident prediction and prevention studies.

References

1) Stoker, J. J. (1957). "Water Waves.", Wiley and Sons, New York, U. S. A.

2) Tetzlaff, D. M., and Harbaugh, J. W. (1989). "Simulating Clastic Sedimentation.", Van Nostrand Reinhold, New York, 202 p.